J Mater Sci (2017) 52:1469–1476

First investigation of the electrochemical performance of γ-$LiFeO_2$ micro-cubes as promising anode material for lithium-ion batteries

Sheng-Ping Guo[1,2,*], Ze Ma[1], Jia-Chuang Li[1], and Huai-Guo Xue[1]

[1] College of Chemistry and Chemical Engineering, Yangzhou University, Yangzhou 225002, Jiangsu, People's Republic of China
[2] State Key Laboratory of Structural Chemistry, Fujian Institute of Research on the Structure of Matter, Chinese Academy of Sciences, Fuzhou 350002, Fujian, People's Republic of China

Received: 28 July 2016
Accepted: 22 September 2016
Published online: 4 October 2016

ABSTRACT

The γ-$LiFeO_2$ micro-cubes were synthesized using a simple solid-state method. Their electrochemical performance as anode material for lithium ion batteries was firstly investigated. Pure γ-$LiFeO_2$ without nanosizing or carbon coating can deliver the first discharge capacity of 1055.3 mAh/g, and 611.5 mAh/g can be maintained after 50 cycles, around 80 % of the second discharge capacity. γ-$LiFeO_2$ also demonstrates nice rate capabilities. These results indicate that γ-$LiFeO_2$ is a promising anode material candidate for lithium ion batteries. The charge/discharge mechanism was also investigated.

Introduction

Energy storage and conversion is one of the hottest topics both in the academic and industrial societies [1–3]. Especially, lithium ion batteries (LIBs) are extensively studied because of their versatile advantages, like light weight, no pollution and high energy density. Their electrochemical properties depend largely on the electrochemical activities of the electrode materials. So, it is being continuously interesting to look for new electrode materials to meet the updating requirements for LIBs in modern society.

Lithium intercalation compounds with the formula $LiMO_2$ (*M*: Fe, Co, Ni and Mn) are one type of attractive candidate cathodes for LIBs because of the relatively easy intercalation and de-intercalation of Li^+ ions [4, 5]. Among them, $LiCoO_2$ is one of the most successful cathode materials that has been largely commercialized. However, its intrinsic drawbacks, like less available Co source and toxicity, restrict its further applications. Accordingly, Fe-based electrode materials should be promising because of the more available and non-toxic Fe source [6–10].

Until now, there are ten polymorphs of $LiFeO_2$ have been discovered as listed in Table 1 and Fig. 1. They are: (1) α-$LiFeO_2$ (*Fm*-3*m*[1], Pearson code *cF*8)

[1] Almost all the literature described the space group of α-$LiFeO_2$ as *Fm*3*m*, however, *Fm*-3*m* should be the right assignment after careful check of the data from inorganic crystal structure data (ICSD), Pearson's crystal data (PCD) and related literature

Address correspondence to E-mail: spguo@yzu.edu.cn

DOI 10.1007/s10853-016-0441-3

Table 1 Structure information of known $LiFeO_2$ polymorphs

Type	Cryst. sys.	Space group	Pearson code	Structure type	References
α-$LiFeO_2$	Cubic	*Fm-3m*	*cF*8	NaCl	[11]
β-$LiFeO_2$	Tetragonal	*I*4/*mmm*	*tI*4	CoO	[12]
β'-$LiFeO_2$	Monoclinic	*C*2/*c*	*mS*32	$NaErO_2$	[12]
γ-$LiFeO_2$	Tetragonal	$I4_1/amd$	*tI*16	–	[12]
Layered $LiFeO_2$	Rhombohedral	*R-3m*	*hR*12	α-$NaFeO_2$	[13, 14]
Goethite-type $LiFeO_2$	Orthorhombic	*Pbnm*	*oP*12	α-FeOOH	[15]
Hollandite-type $LiFeO_2$	Tetragonal	*I*4/*m*	*tI*24	β-FeOOH	[15]
Corrugated layer $LiFeO_2$	Orthorhombic	*Pmmn*	*oP*8	β-$NaMnO_2$	[16]
Ordered rock-salt $LiFeO_2$	Cubic	*Fd-3m*	*cF*64	$LiTiO_2$	[11, 14]
Tetrahedral *T*-$LiFeO_2$	Orthorhombic	$Pna2_1$	*oP*16	β-$NaFeO_2$	[17]

with the cubic NaCl-type structure;[8] (2) β-$LiFeO_2$ (*I*4/*mmm*, Pearson code *tI*4) with the tetragonal CoO-type structure;[9] (3) β'-$LiFeO_2$ (*C*2/*c*, Pearson code *mS*32) with the monoclinic $NaErO_2$-type structure;[9] (4) γ-$LiFeO_2$ ($I4_1/amd$, Pearson code *tI*16) with novel tetragonal structure [12]; (5) layered $LiFeO_2$ (*R-3m*, *hR*12) with the rhombohedral α-$NaFeO_2$-type structure [13, 14]; (6) goethite-type $LiFeO_2$ (*Pbnm*, *oP*12) with the α-FeOOH-type structure [15]; (7) hollandite-type $LiFeO_2$ (*I*4/*m*, *tI*24) with the β-FeOOH-type structure [15]; (8) corrugated layer $LiFeO_2$ (*Pmmn*, *oP*8) with the orthorhombic β-$NaMnO_2$-type structure [16]; (9) ordered rock-salt $LiFeO_2$ (*Fd-3m*, *cF*64) with the $LiTiO_2$-type structure [11, 14] and (10) *T*-$LiFeO_2$ ($Pna2_1$, *oP*16) with the orthorhombic β-$NaFeO_2$-type structure [17]. Among them, only several of them have been reported being electrochemical-active. Especially for α-$LiFeO_2$, its electrochemical behaviors have been investigated extensively. While for γ-$LiFeO_2$, a superstructure polymorph of α-$LiFeO_2$, its electrochemical performance was particularly depressed when it was employed as the cathode material for LIBs [12, 15].

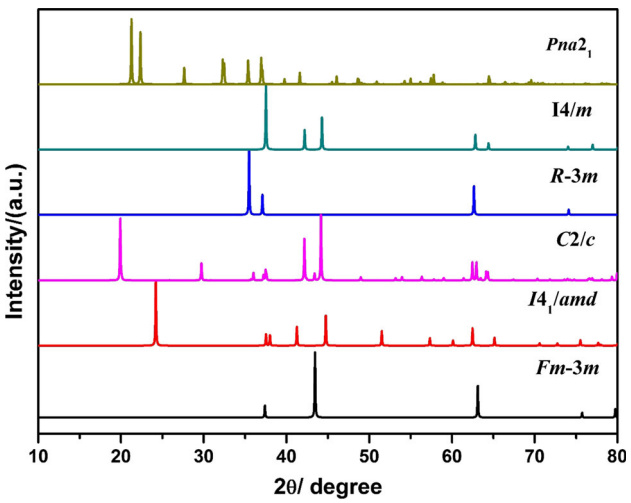

Figure 1 The powder X-ray diffraction patterns of known polymorphs of $LiFeO_2$. Only crystal structure data for six polymorphs of $LiFeO_2$ can be found.

It is well known that transition-metal oxides are one type of most promising anode materials for LIBs [18, 19], and iron oxides have attracted much interest among them because of the advantages of Fe element [20–22]. Comparing $LiFeO_2$ with Fe_2O_3, it is possible to employ the former as anode material, too. In fact, there are several reports about the application of α-$LiFeO_2$ as anode recently. [23–27]. However, so far, there is no such study on γ-$LiFeO_2$, which may be caused by the facts that γ-$LiFeO_2$ has very bad electrochemical performance and γ-phase can't be experimentally easily available.

Recently, γ-$LiFeO_2$ micro-cubes were occasionally obtained by us using a simple solid state method. Later on, the synthesis method was optimized and pure γ-$LiFeO_2$ micro-cubes could be obtained reproducibly. Here, the synthesis, various characterizations and electrochemical performance of γ-$LiFeO_2$ as the anode material for LIB are firstly reported and discussed.

Experimental

Synthesis and material characterization

Pure γ-$LiFeO_2$ was synthesized using a facile solid state method. 158.2 mg Li_2CO_3 (99.0 %, aladdin) and 341.8 mg Fe_2O_3 (99.9 %, aladdin) with the molar ratio of 1:1 were mixed, ground to a fine powder and pressed to a pellet, then the pellet was placed into a corundum crucible, heated in a muffle furnace from

room temperature to 600°C in 4 hours and maintained for 48 hours.

Powder X-ray diffraction (PXRD, Bruker D8 Advance) pattern was collected at 40 kV and 100 mA for Cu$K\alpha$ radiation ($\lambda = 1.5406$ Å) with a scan speed of 5°/minutes. Field emission scanning electron microscopy (FE-SEM, Hitachi S-4800II) and transmission electron microscopy (TEM, Philips Tecnai12) were used to investigate the sample's morphology. Raman spectra (Renishaw inVia) measurement was done assuming a linear baseline in the spectral range 200–2000 cm^{-1}.

Electrochemical characterization

The electrode slurry was prepared using γ-$LiFeO_2$, super C65 and polyvinylidene fluoride (PVDF) with the molar ratios of 7: 2: 1 dissolved in *N*,*N*-2-methyl pyrrolidone (NMP). The slurry was magnetically stirred for 1 day, then it was coated onto a Cu foil, dried at 120 °C for overnight using a vacuum drying oven and cut the dried foil into Φ1.6 cm disks. The weight of electrode material is around 3 mg. The CR-2032 type coin cell was assembled using a Li foil as the counter electrode and a Celgard 2325 film as the separator in a glovebox filled with argon. The electrolyte used was 1 M $LiPF_6$ in a mixed solvent of DEC and EC with a volume ratio of 1:1. The galvanostatic charge/discharge tests were carried out at a constant current density of 0.1 C in the potential range of 0.01–3 V using NEWARE CT-3008 charge–discharge system. The cells were first discharged to 0.01 V, and then the cycle number was counted. Cyclic voltammetry (C–V) (electrochemical workstation, CHI660D) curves were measured in 0.01–3 V with the scan rate of 0.5 mV/s.

Results and discussion

It has to be mentioned that the synthesis of γ-$LiFeO_2$ has to be handled very seriously. Even small adjustment of the heating profiles, the ratios of the raw materials and the insufficient grind would result in the failure to get γ-phase. The solid-state method employed here is really simple, and scalable γ-$LiFeO_2$ micro-cubes could be obtained without any impurities.

The crystal structure of γ-$LiFeO_2$ is shown in Fig. 2. It crystallizes in the tetragonal space group $I4_1/amd$ representing a new structure type with Pearson symbol *tI*16. There is only one Fe, one Li and one O atom in its crystallographically independent unit. Both metal atoms coordinate with six O atoms to form distorted octahedra. Each FeO_6 octahedron shares edge with four FeO_6 octahedra and corner with the other four FeO_6 octahedra. The whole structure can be described as FeO_6 octahedra constructed 3-D network and Li^+ ions occupy the octahedral interspaces.

The PXRD pattern (Fig. 3) confirms that the as-prepared sample is pure γ-$LiFeO_2$ as the measured one is well matched with the calculated one. The calculated PXRD pattern is simulated from the structure data of γ-$LiFeO_2$ (ICSD No. 174086). The SEM image (Fig. 4a) indicate that the γ-$LiFeO_2$ particles are cube-like with the diameter around 100–300 nm, while most of them are less than 200 nm. The high resolution TEM image (Fig. 4b) showing the uneven sizes of γ-$LiFeO_2$ cubes are in good agreement with the SEM images. The lattice fringes of γ-$LiFeO_2$ micro-cubes are obviously visible (Fig. 4c).

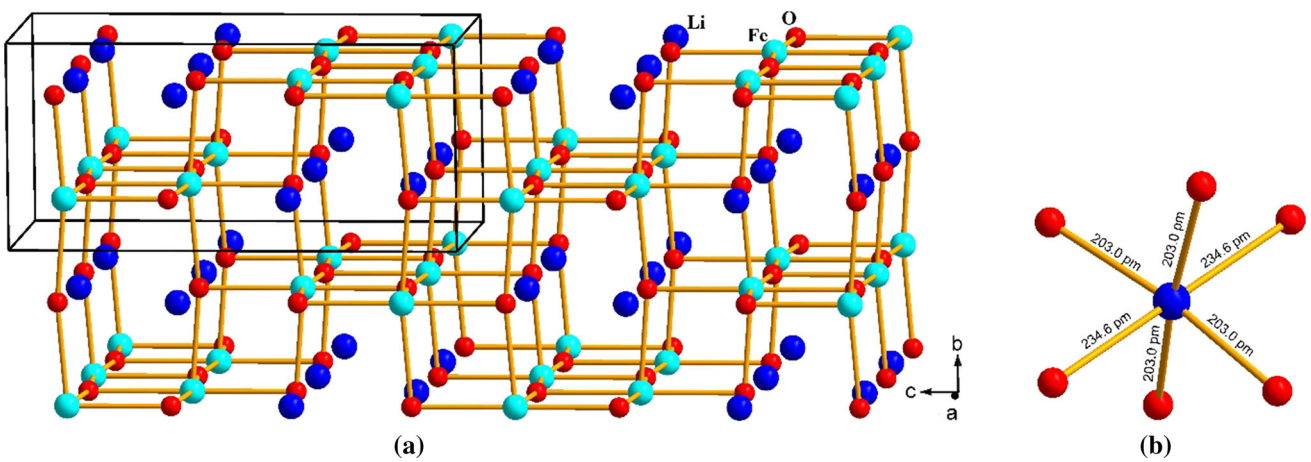

Figure 2 Crystal structure of γ-$LiFeO_2$.

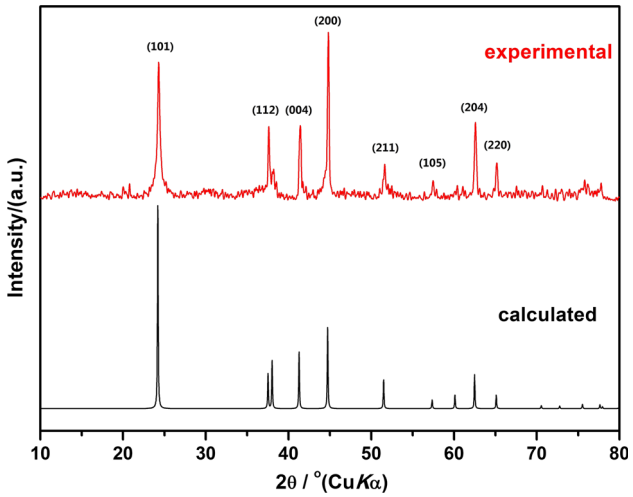

Figure 3 PXRD pattern of γ-$LiFeO_2$.

The charge–discharge curves of γ-$LiFeO_2$ (Fig. 5) for the first three cycles indicate the work potential is around 1.1 V vs Li^+/Li, close to the value of α-$LiFeO_2$ [23–27]. The Coulombic efficiencies of γ-$LiFeO_2$, Fe_2O_3 and Fe_3O_4 is 72.89, 68.30 and 51.66 % in the first cycle, indicating that it can effectively increase the first cycle's Coulombic efficiency via compensating the lithium loss in the first cycle by adding some lithium into the anode, namely, from iron oxides to $LiFeO_2$. Further, the Coulombic efficiency of γ-$LiFeO_2$ is close to 100 % during the following cycles.

The cycling data at 0.1 C (Fig. 6) shows that the initial discharge capacity can be reached to 1055.3 mAh/g, higher than its theoretical capacity of 848 mAh/g. However, the first charge capacity is only 769.2 mAh/g, indicating that there is irreversible 286.1 mAh/g capacity loss. The discharge and charge capacities after the first cycle are reduced to 765.2 and 725.4 mAh/g, respectively. After the 50th cycle, there is 611.5 mAh/g capacity residual, which is 79.9 % of the 2nd cycle's value. Except for the first cycle, the Coulombic efficiencies are very close to 100 % for all the 50 cycles, indicating its excellent reversible electrochemical reactions.

Compared to the electrochemical results of α-$LiFeO_2$ as anode material, γ-$LiFeO_2$'s capacity after 50 cycles is lower than those values of α-$LiFeO_2$ and α-$LiFeO_2$/C nanofibers with 3-D nano-architectures [23]; however, the capacity retention of γ-$LiFeO_2$ is better. The lower capacity should be ascribed to the pristine γ-$LiFeO_2$ without any nanosizing or carbon coating. We also tried to prepare the γ-$LiFeO_2$/C composite, however, γ-phase was failed to be obtained once the carbon material introduced. The further optimization of the electrochemical performance of γ-$LiFeO_2$ is still underway.

The rate performance of γ-$LiFeO_2$ (Fig. 7) was studied at rates from 0.1 to 10 C with the interval of ten cycles, and finally return to 0.1 C. The highest discharge capacities are 1018, 660, 563, 428, 399, 378, 185, 68 and 705 mAh/g at 0.1, 0.2, 0.4, 0.8, 1, 2, 5, 10 and 0.1 C, respectively. When return to 0.1 C, the capacity can be recovered to 700 mAh/g, much close to the value attained without high-rate measurement.

The C-V (Fig. 8) measurements for the first three curves were recorded in 0.01–3 V. For the first cycle, the cathodic peak appears at around 0.55 V, lower than that of α-$LiFeO_2$ and caused by the reduction of Fe^{3+} to Fe, the corresponding electrochemical

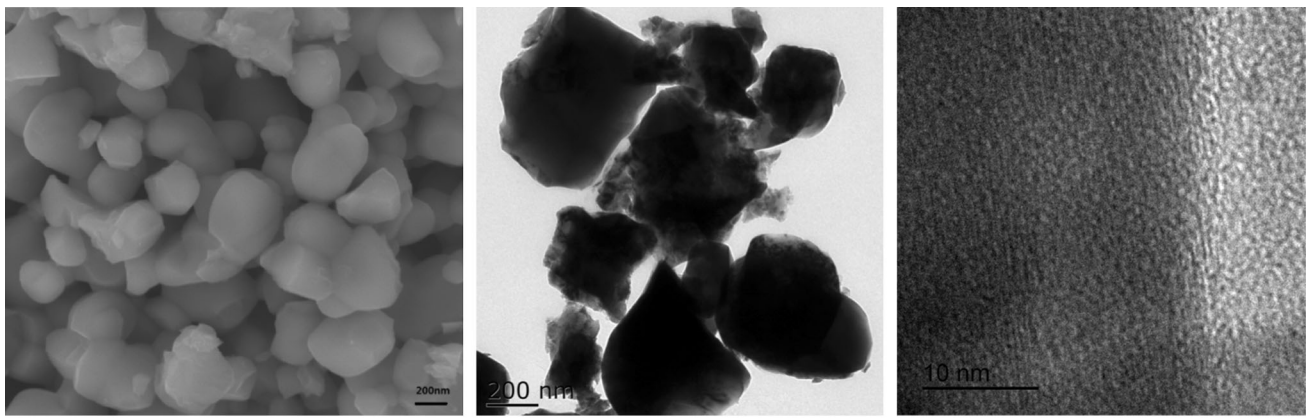

Figure 4 The SEM (**a**) and TEM (**b**, **c**) images of γ-$LiFeO_2$ micro-cubes.

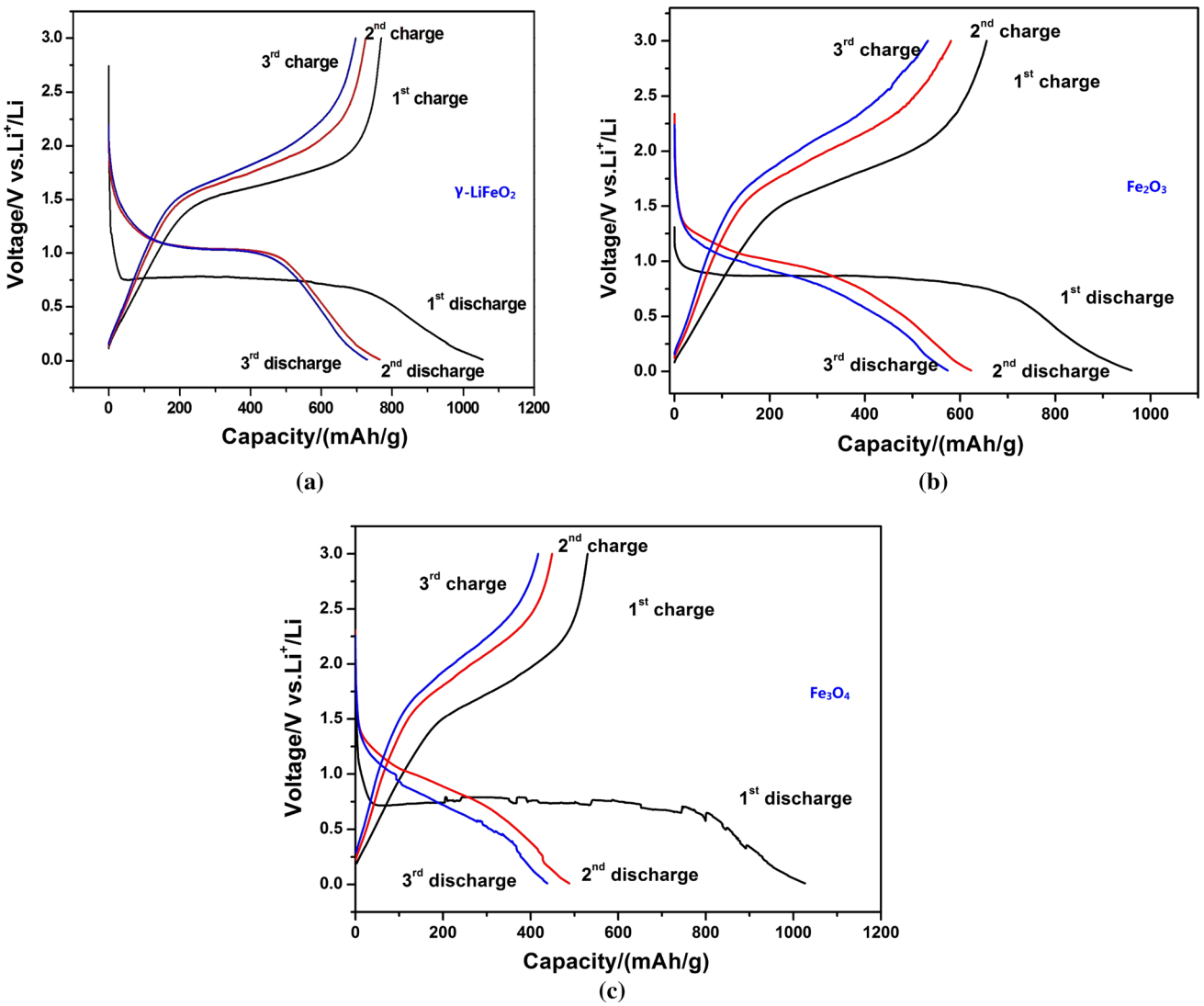

Figure 5 The galvanostatic charge/discharge curves of γ-$LiFeO_2$ (**a**), Fe_2O_3 (**b**) and Fe_3O_4 (**c**) for the first three cycles.

reaction can be expressed as the reaction γ-$LiFeO_2 + 3e^- + 3Li^+ \rightarrow 2Li_2O + Fe$ [23–27]. The broad oxidation peak appeared at around 1.70 V, which might be consisted of two neighboring peaks according to its shape. It corresponds to the oxidation of Fe^0 to Fe^{2+}, and further to Fe^{3+} [23–27]. After the 1st cycle, γ-$LiFeO_2$ demonstrates nice electrochemical reversibility as evidenced by the almost completely overlap of the C–V curves for the 2nd and 3rd cycles. The cathodic peak moves to 0.92 V for the latter two cycles, while the anodic peak keeps almost voltage unchanged, just the shape altered. Comparing the first three C–V curves of γ- and α-$LiFeO_2$, it can be concluded that their shapes are similar, just the cathodic peaks' locations are a little different. The subtle difference between the electrochemical mechanisms for γ-$LiFeO_2$ and α-$LiFeO_2$ might not be explained from their crystal structures, as the former has much worse electrochemical behavior than that of the latter when employed as cathode materials.

To better understand the first charge and discharge mechanism, two cells only undergone the first discharge and the first cycle, respectively, were opened and washed to get the anode materials, scraped the active materials from the copper foil, which were then subsequently characterized by powder XRD measurements. As shown in Fig. 9a, both the XRD peaks after first discharge and first charge become amorphous. Considering the C–V curves' similarity of α- and γ-$LiFeO_2$ after the first cycle, it could be presumed that γ-$LiFeO_2$ should be amorphous after the first cycle, too. These results are also verified by the Raman spectra

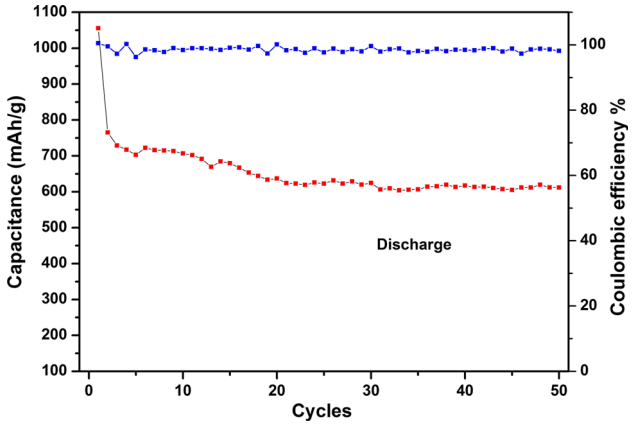

Figure 6 The cycling performance of γ-$LiFeO_2$ at 0.1 C.

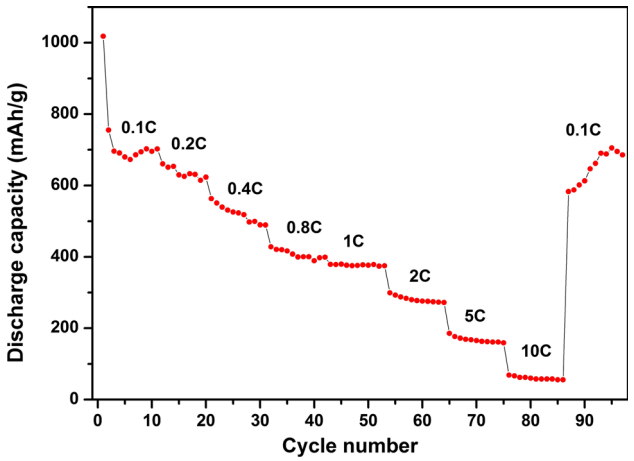

Figure 7 The rate performance of γ-$LiFeO_2$.

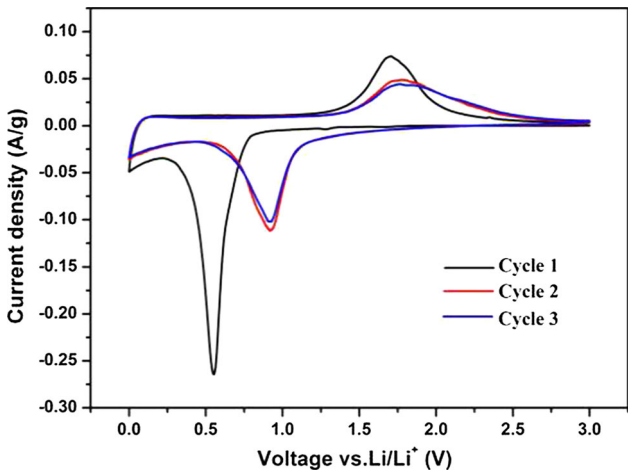

Figure 8 The C–V *curves* of γ-$LiFeO_2$.

(Fig. 9b). It shows the existence of γ-$LiFeO_2$ and carbon before electrochemical measurement, and the Raman peaks of γ-$LiFeO_2$ disappeared after the first cycle.

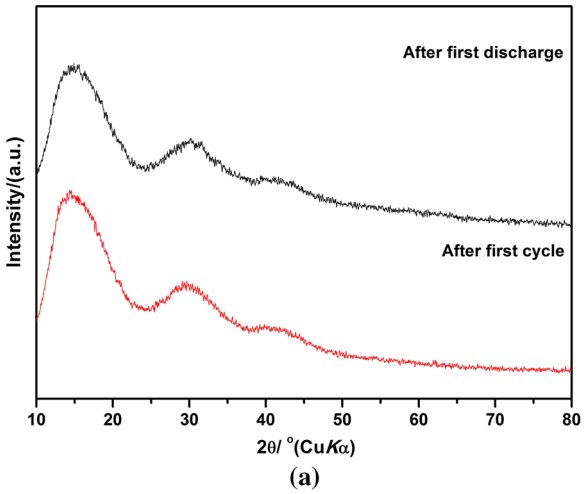

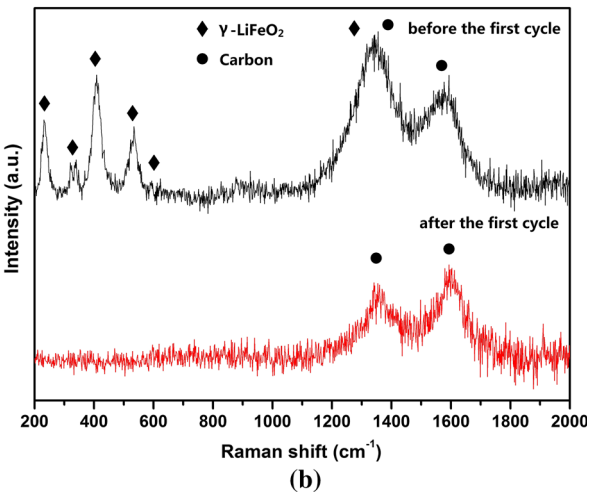

Figure 9 **a** PXRD patterns of γ-$LiFeO_2$ after the first discharge (*black*) and first cycle (*red*). **b** Raman spectra of γ-$LiFeO_2$ before (*black*) and after (*red*) the first cycle.

The subtle difference between the electrochemical mechanisms for γ-$LiFeO_2$ and α-$LiFeO_2$ might not be explained from their crystal structures, as the former has much worse electrochemical behavior than that of the latter when employed as cathode materials. Here, the electrochemical data of γ-$LiFeO_2$ as anode material was firstly studied with focusing on its facile synthesis method and promising electrochemical behavior.

Conclusion

In summary, a simple solid-state method was employed to synthesize γ-$LiFeO_2$ micro-cubes. γ-$LiFeO_2$ firstly studied here as the anode material

demonstrates promising electrochemical behaviors. Without nanosizing or carbon coating efforts, it has the first discharge capacity of 1055.3 mAh/g, and 611.5 mAh/g can be maintained after 50 cycles, around 80 % of the second discharge capacity. It can be expected that its electrochemical performance will be largely enhanced through nano- or doping techniques. The electrochemical study of γ-$LiFeO_2$ is still in its infancy. We hope this work can stimulate more studies on various polymorphs of "cathode material" $LiFeO_2$ used as anode material for LIBs.

Acknowledgements

We gratefully acknowledge the financial support by National Natural Science Foundation of China (Grant No. 21173183), the Higher Education Science Foundation of Jiangsu Province (No. 15KJB150031), State Key Laboratory of Structural Chemistry Fund (No. 20150009), the Priority Academic Program Development of Jiangsu Higher Education Institutions and the Qing Lan project. We would also like to acknowledge the technical support received from the Testing Center of Yangzhou University.

References

[1] Trogadas P, Ramani V, Strasser P, Fuller TF, Coppens MO (2015) Hierarchically structured nanomaterials for electrochemical energy conversion. Angew Chem Int Ed 54:122–148

[2] Vlad A, Singh N, Galande C, Ajayan PM (2015) Design considerations for unconventional electrochemical energy storage architectures. Adv Energy Mater 5:201402115

[3] Hu CG, Song L, Zhang ZP, Chen N, Feng ZH, Qu LT (2015) Tailored graphene systems for unconventional applications in energy conversion and storage devices. Energy Environ Sci 8:31–54

[4] Wu NT, Zhang Y, Guo Y, Liu SJ, Liu H, Wu H (2016) Flakelike $LiCoO_2$ with exposed 010 facets as a stable cathode material for highly reversible lithium storage. ACS Appl Mater Interfaces 8:2723–2731

[5] He P, Yu HJ, Li D, Zhou HS (2012) Layered lithium transition metal oxide cathodes towards high energy lithium-ion batteries. J Mater Chem 22:3680–3695

[6] Kang B, Ceder G (2009) Battery materials for ultrafast charging and discharging. Nature 458:190–193

[7] Barpanda P, Nishimura S, Yamada A (2012) High-voltage pyrophosphate cathodes. Adv Energy Mater 2:201100772

[8] Yan MY, Zhang GB, Mai LQ (2016) In operando observation of temperature dependent phase evolution in lithium-incorporation olivine cathode. Nano Energy 22:406–413

[9] Zhang L, Xiang HF, Wang HH (2012) Synthesis of $LiFePO_4$/C composite as a cathode material for lithium-ion battery by a novel two-step method. J Mater Sci 47:3076–3081

[10] Muruganantham R, Sivakumar M, Subadevi R, Wu NL (2015) A facile synthesis and characterization of $LiFePO_4$/C using simple binary reactants with oxalic acid by polyol technique and other high temperature methods. J Mater Sci Mater Electron 26:2095–2106

[11] Vucinic-Vasic M, Antic B, Blanusa J, Rakic S, Kremenović A, Nikolic AS, Kapor A (2006) Formation of nanosize Li-ferrites from acetylacetonato complexes and their crystal structure, microstructure and order-disorder phase transition. Appl Phys A 82:49–54

[12] Barré M, Catti M (2009) Neutron diffraction study of the β' and γ Phases of $LiFeO_2$. J Solid State Chem 182:2549–2554

[13] Chappel E, Holzapfel M, Chouteau G, Ott A (2000) Effect of cobalt on the magnetic properties of the $LiFe_{1-x}Co_xO_2$-layered system ($0 \le x \le 1$). J Solid State Chem 154:451–459

[14] Hirayama M, Tomita H, Kubota K, Kanno R (2011) Structure and electrode reactions of layered rocksalt $LiFeO_2$ nanoparticles for lithium battery cathode. J Power Sources 196:6809–6814

[15] Li JG, Li JJ, Luo J, Wang L, He XM (2011) Recent advances in the $LiFeO_2$-based materials for Li-ion batteries. Int J Electrochem Sci 6:1550–1561

[16] Catti M, Montero-Campillo M (2011) Lithium diffusion pathways and vacancy formation in the Pmmn $Li_{1-x}FeO_2$ electrode material. Phys Chem Chem Phys 13:11156–11164

[17] Armstrong AR, Tee DW, Mantia FL, Novák P, Bruce PG (2008) Synthesis of tetrahedral $LiFeO_2$ and its behavior as a cathode in rechargeable lithium batteries. J Am Chem Soc 130:3554–3559

[18] Jiang J, Li YY, Liu JP, Huang XT, Yuan CZ, Lou XW (2012) Recent advances in metal oxide-based electrode architecture design for electrochemical energy storage. Adv Mater 24:5166–5180

[19] Yu XG, Marks TJ, Facchetti A (2016) Metal oxides for optoelectronic applications. Nature Mater 15:383–396

[20] Zhou H, Ruther RE, Adcock J, Zhou W, Dai S, Nanda J (2015) Controlled formation of mixed nanoscale domains of high capacity Fe_2O_3–FeF_3 conversion compounds by direct fluorination. ACS Nano 9:2530–2539

[21] An QY, Lv F, Liu QQ, Han CH, Zhao KN, Sheng JZ, Wei QL, Yan MY, Mai LQ (2014) Amorphous vanadium oxide matrixes supporting hierarchical porous Fe_3O_4/graphene

nanowires as a high-rate lithium storage anode. Nano Lett 14:6250–6256

[22] Du DJ, Yue WB, Ren Y, Yang XJ (2014) Fabrication of graphene-encapsulated CoO/$CoFe_2O_4$ composites derived from layered double hydroxides and their application as anode materials for lithium-ion batteries. J Mater Sci 49:8031–8039

[23] Büyükyazi M, Mathur S (2015) 3D nanoarchitectures of α-$LiFeO_2$ and α-$LiFeO_2$/C nanofibers for high power lithium-ion batteries. Nano Energy 13:28–35

[24] Obrovac MN, Dunlap RA, Sanderson RJ, Dahn JR (2001) The electrochemical displacement reaction of lithium with metal oxides. J Electrochem Soc 148:A576–A588

[25] Krummacher J, Passerini S, Balducci A (2015) Ionic liquid assisted solid-state synthesis of lithium iron oxide nanoparticles for rechargeable lithium ion batteries. Solid State Ionics 280:37–43

[26] Rahman MM, Wang JZ, Hassan MF, Chen ZX, Liu HK (2011) Synthesis of carbon coated nano crystalline porous α-$LiFeO_2$ composite and its application as anode for the lithium ion battery. J Alloys Compd 509:5408–5413

[27] Li KY, Chen H, Shua FF, Xue DF, Guo XW (2014) Facile synthesis of iron-based compounds as high performance anode materials for Li-ion batteries. RSC Adv 4:36507–36512